Proceedings of the Thirty-sixth (2026) International Ocean and Polar Engineering Conference **www.isope.org**
Orlando, Florida, USA, May 31-June 5, 2026

ISBN 978-1-880653-72-2; ISSN 1098-6189

A Deep-Learning Approach for Super-Resolution Reconstruction of Wind Turbine Wakes in Atmospheric Boundary Layers

Maokun Ye[1], Hanqiao Han[2], Mingqiu Liu[1], Decheng Wan[1]*

[1] Computational Marine Hydrodynamics Lab (CMHL), School of Ocean and Civil Engineering
Shanghai Jiao Tong University, Shanghai, China
[2] Wuhan Second Ship Design and Research Institute, Wuhan, China
[*]Corresponding author

ABSTRACT

Wind turbine wake interactions significantly impact wind farm efficiency, necessitating accurate wake monitoring for layout optimization and power loss mitigation. However, conventional approaches—including analytical models, computational fluid dynamics simulations, and field measurements—face limitations in balancing computational cost, spatial resolution, and real-time applicability. This study introduces a deep learning-based super-resolution framework to reconstruct high-fidelity wake fields from sparse, low-resolution data, mimicking practical lidar outputs. Leveraging a U-Net architecture, the model learns nonlinear mappings between down-sampled inputs and high-resolution targets derived from large eddy simulations of a utility-scale turbine operating in a neutral atmospheric boundary layer. The proposed method effectively captures critical wake features, such as velocity deficits and turbulence gradients, surpassing traditional interpolation techniques in qualitative and quantitative assessments. By demonstrating robust performance across varying data sparsity levels, this work establishes a novel pathway for real-time wake reconstruction, with potential applications in adaptive turbine control and wind farm management for both onshore and offshore environments, where sparse monitoring constraints and wake-induced power losses are more pronounced. Future directions include extending the approach to complex atmospheric conditions, offshore marine boundary layer scenarios, and experimental validation with field lidar measurements from onshore and offshore wind farms.

KEY WORDS: Wind turbine wake; Super-resolution reconstruction; CFD; Data-Driven; Machine-learning

INTRODUCTION

Wind turbine wake monitoring and assessment are foundational to optimizing wind farm layout, operational efficiency, and component lifespan, as wake interactions between turbines can reduce power output by up to 20–30% in densely packed farms, with even more pronounced impacts in offshore wind farms due to longer wake recovery distances over the low-roughness sea surface. Three primary approaches are currently used for wake evaluation: analytical wake models, computational fluid dynamics (CFD) simulations, and field measurements (Amiri et al. 2024). Analytical wake models, such as the Jensen or Bastankhah models (Bastankhah and Porté-Agel 2014), are widely employed in preliminary design due to their computational efficiency, but they rely on simplified empirical assumptions that fail to capture the nonlinear dynamics of wake turbulence and atmospheric boundary layer (ABL) interactions. Field measurements (Chen et al. 2025), using lidars or sodars, provide ground-truth data but are limited by high deployment costs, spatial coverage constraints, and sensitivity to weather conditions. CFD simulations, by contrast, offer high-fidelity spatial and temporal resolution of flow fields (Xu et al. 2022; Ye et al. 2023; Ye et al. 2024; Ye et al. 2026), enabling detailed analysis of wake evolution. Despite these advantages, CFD simulations are computationally expensive and time-consuming—requiring days or weeks for large-scale wind farm simulations—making them unsuitable for real-time wake forecasting or adaptive turbine control. This limitation is even more restrictive for offshore wind farms, where large spatial scales and complex coupled wind-wave-current-mooring loads further elevate the computational cost of high-fidelity CFD simulations.

To enable real-time operational decision-making, wind farms increasingly deploy remote sensing instruments like scanning lidars, which provide continuous wind speed and direction measurements. However, these devices generate sparse, low-resolution data, as they sample flow fields along discrete lines or points rather than capturing full spatial coverage (Ali et al. 2021; Ye et al. 2026). This sparsity poses a critical challenge: reconstructing a high-fidelity wake field from limited observations is essential for quantifying wake-induced power losses and guiding yaw control or de-rating strategies, yet traditional interpolation techniques (e.g., bicubic interpolation) often smooth out critical flow features such as velocity deficits and turbulence gradients, leading to inaccurate wake assessments.

In recent years, deep learning-based super-resolution (SR) techniques have emerged as a promising solution for reconstructing high-resolution flow fields from low-resolution inputs (Deng et al. 2019; Chen 2023; Ye et al. 2025). Convolutional neural networks (CNNs) (Lecun et al. 2015) and U-Net architectures, in particular, have been successfully applied to enhance the resolution of CFD datasets for applications ranging from airfoil aerodynamics to urban airflow. For example, researchers have used U-Net models to reconstruct high-resolution turbulent boundary layers from coarse-grid CFD outputs, demonstrating superior performance over traditional interpolation methods in preserving flow physics. However, most existing studies focus on generic flow fields or idealized wake scenarios, with limited attention to the unique challenges of wind turbine wakes under realistic ABL conditions—where the interaction between ABL turbulence and wake dynamics introduces complex, spatially varying flow features that are difficult to capture with simplified models.

This paper presents a data-driven deep learning approach for reconstructing high-fidelity wind turbine wake fields from sparse, low-resolution measurements, mimicking the output of lidar systems. The proposed method leverages a U-Net (Ronneberger et al. 2015) architecture to learn the nonlinear mapping between down-sampled, low-resolution flow field inputs (representing sparse lidar observations) and high-resolution CFD-derived wake fields (generated from precursor simulations of neutral ABLs). By training the model on realistic, physics-informed data, we aim to enable real-time wake reconstruction that captures the intricate dynamics of ABL-wake interactions.

The key contributions of this work are threefold. First, it represents the first systematic effort to integrate super-resolution techniques with the practical challenge of wind turbine wake monitoring, demonstrating how a U-Net model can effectively capture the nonlinear flow physics of wakes evolving within neutral atmospheric boundary layers. Second, the study uses high-fidelity CFD datasets generated from precursor simulations, ensuring that the training data reflects realistic inflow conditions and wake dynamics rather than idealized assumptions. Finally, by evaluating model performance across two down-sampling rates (DSR = 16 and DSR = 32) and comparing results against bicubic interpolation, this work provides a rigorous assessment of the model's ability to preserve critical wake features—including velocity deficits and turbulence intensity—even with highly sparse input data.

The remainder of this paper is organized as follows: Section 2 details the generation of the high-fidelity CFD dataset, including the test-case setup for the NREL 5MW turbine, precursor simulation of the neutral ABL, and numerical methodology. Section 3 defines the U-Net architecture and formulates the super-resolution problem for wake reconstruction. Section 4 outlines the model training procedure, including data down-sampling, dataset splitting, and training specifications. Section 5 presents and discusses the reconstruction results for both down-sampling rates, alongside quantitative and qualitative comparisons with bicubic interpolation. Finally, Section 6 summarizes the key findings and proposes directions for future research.

GENERATION OF HIGH-FIDELITY DATASET

For data-driven deep learning models, the quality and physical authenticity of training datasets are pivotal to their performance in practical applications. A high-fidelity dataset that accurately reflects the dynamic characteristics of wind turbine wakes and atmospheric boundary layer (ABL) interactions can effectively enhance the generalization ability of the proposed U-Net model, ensuring that the trained model can reliably reconstruct real wake fields. This chapter comprehensively elaborates on the entire process of dataset generation, including test-case design, CFD numerical methodology, detailed simulation setup, and analysis of CFD results, providing a solid foundation for subsequent model training and validation.

Test-Case Description

To ensure the rationality, comparability, and engineering applicability of the research, the NREL 5MW reference wind turbine was selected as the test object in this study. As a widely recognized benchmark model in the field of wind energy research, this turbine's structural and operational parameters have been standardized and documented in detail, making it an ideal choice for wake simulation and model validation (Jonkman et al. 2009). The key operational and structural parameters of the turbine are as follows: the rated wind speed is 11.4 m/s, the rated rotational speed reaches 12.1 rpm, the rotor diameter (D) is 126 m, and the hub height is set to 90 m. These parameters are consistent with the typical configuration of utility-scale wind turbines for both onshore and offshore applications (Jonkman et al. 2009), ensuring that the simulated wake characteristics are representative of practical engineering scenarios in both land-based and marine environments.

The inflow condition for the wind turbine was designed as a neutral ABL, which is one of the most common and representative atmospheric states in wind farm operations. A neutral ABL is characterized by a negligible vertical temperature gradient, meaning that buoyancy effects can be ignored in the flow field simulation, and the flow evolution is mainly dominated by shear stress and turbulent mixing. To simulate the turbine's typical operational state, the mean wind speed at the hub height was precisely set to 11.4 m/s, which matches the rated wind speed of the NREL 5MW turbine. This configuration ensures that the generated wake exhibits obvious nonlinear dynamic characteristics, such as significant velocity deficit, wake expansion, and turbulent diffusion, which are essential for training the super-resolution model to capture fine-scale flow features.

CFD Methodology

To obtain high-fidelity flow field data of wind turbine wakes under neutral ABL conditions, a two-stage numerical simulation strategy based on Large Eddy Simulation (LES) was adopted in this study. This strategy combines precursor simulation and wake simulation, which can effectively generate a fully developed neutral ABL and accurately simulate the interaction between the ABL and wind turbine wakes, overcoming the limitations of traditional single-stage simulation in reproducing realistic inflow conditions.

LES was selected as the computational paradigm for wake simulation. Unlike Reynolds-Averaged Navier-Stokes (RANS) methods that average turbulent fluctuations over time, LES achieves scale separation of turbulent structures: large-scale turbulent eddies (which directly dominate wake evolution, vortex shedding, and energy transfer) are directly solved by numerically integrating the filtered Navier-Stokes equations, while small-scale subgrid turbulence (which has a negligible impact on wake macro characteristics) is modeled using a subgrid-scale (SGS) stress closure model. This approach ensures that the simulation can capture the fine temporal and spatial details of wake flow fields, which is crucial for generating high-quality training data for the super-resolution model. In the LES framework, the spatial filter scale Δ is defined as the geometric mean of the grid cell dimensions in the streamwise (x), cross-flow (y), and vertical (z) directions, which is expressed as $\Delta = \left(\Delta_x \Delta_y \Delta_z\right)^{1/3}$ where Δ_x, Δ_y, and Δ_z are the grid cell sizes in the three orthogonal directions, respectively. The filtered governing equations for incompressible flow in the LES model include the continuity equation and the momentum equation, which comprehensively consider the key physical effects such as turbine aerodynamic forces, Coriolis effects, and atmospheric pressure gradients. The specific forms of the equations are as follows:

$$\frac{\partial u_i}{\partial x_i} = 0 \tag{1}$$

$$\begin{aligned}\frac{\partial u_i}{\partial t} + \frac{\partial\left(u_j u_i\right)}{\partial x_j} = &-\frac{\partial p}{\partial x_i} - \frac{\partial \tau_{ij}^D}{\partial x_j} - \frac{1}{\rho_0}\frac{\partial p_0(x, y)}{\partial x_i} \\ &+ g\left(\frac{\theta - \theta_0}{\theta_0}\right)\delta_{i3} - 2\varepsilon_{i3k}\Omega_3 u_k + \frac{F_i}{\rho_0}\end{aligned} \tag{2}$$

In the above equations, t denotes time; u_i represents the filtered velocity components ($i = 1,2,3$ corresponding to the x, y, z directions respectively); p is the modified pressure; ρ_0 is the reference air density; F_i is the aerodynamic force exerted by the wind turbine on the flow field; g is the gravitational acceleration; θ is the resolved mean potential temperature;θ_0 is the reference temperature; Ω_3 is the Earth's rotation vector (defined as $\Omega_3 = \omega[0, \cos\varphi, \sin\varphi]$, where ω is the Earth's angular velocity and φ is the geographic latitude of the turbine site); and τ_{ij}^D is the subgrid-scale stress tensor.

The Smagorinsky closure model was adopted to model the subgrid-scale stress tensor τ_{ij}^D, which is a mature and widely used SGS model in LES of turbulent flows. The model assumes that the subgrid-scale stress is proportional to the resolved strain rate tensor, and its specific expression is:

$$\tau_{ij}^D = -2\nu^{SGS} S_{ij} \tag{3}$$

$$\nu^{SGS} = (C_s \Delta)^2 \left(2 S_{ij} S_{ij}\right)^{1/2} \tag{4}$$

where $C_s = 0.13$ is the model constant (determined based on extensive validation in ABL and wake simulations); ν^{SGS} is the subgrid-scale eddy viscosity; and S_{ij} is the resolved strain rate tensor, which is defined as:

$$S_{ij} = \frac{1}{2}\left(\frac{\partial u_i}{\partial x_j} + \frac{\partial u_j}{\partial x_i}\right) \tag{5}$$

The Actuator Line Method (ALM) proposed by Sørensen and Shen (Sørensen and Shen 2002) was employed to model the aerodynamic forces exerted by the wind turbine blades on the flow field. This method abstracts each turbine blade into a series of discrete airfoil elements distributed along the spanwise direction (from the blade root to the tip). For each airfoil element, the aerodynamic lift and drag forces are calculated using blade element theory, which is based on the local relative wind velocity and angle of attack at the element position. To avoid numerical singularities caused by concentrated forces, the calculated aerodynamic forces of each airfoil element are projected onto the surrounding grid cells using a Gaussian smoothing kernel. This smoothing process ensures that the forces are evenly distributed over the adjacent grid cells, maintaining the numerical stability of the simulation while preserving the physical authenticity of the force interaction between the blades and the flow field. The ALM method effectively balances the computational efficiency and accuracy, making it suitable for high-fidelity wake simulation of large-scale wind turbines.

To generate a fully developed neutral ABL as the inflow condition for wind turbine wake simulation, a two-stage computational strategy was implemented (Lee et al. 2012), as shown in Fig. 1. The first stage is the precursor LES, which aims to develop a quasi-equilibrium neutral ABL with stable turbulence statistics. During this stage, no wind turbine is included in the computational domain, and the simulation runs for a sufficiently long time (0–18000 s) to ensure that the ABL reaches a fully developed state, with stable velocity profiles and turbulence intensity distributions. The second stage is the wake simulation stage. After the precursor simulation reaches a steady state, the NREL 5MW wind turbine is introduced into the computational domain, and the simulation continues for 300 s (18000–18300 s). The initial conditions (IC) and boundary conditions (BC) for the wake simulation are extracted from the final steady state of the precursor simulation, ensuring that the inflow condition is consistent with the realistic neutral ABL. This two-stage strategy effectively avoids the problem of incomplete ABL development in single-stage simulations, ensuring that the wake evolution characteristics simulated are consistent with practical engineering scenarios.

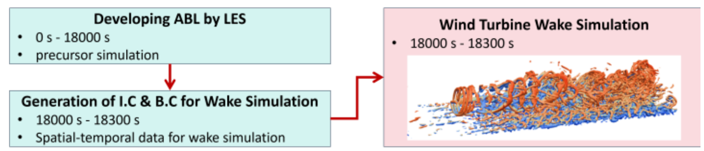

Figure 1. Simulation procedure.

Numerical Setup

The computational domain was designed as a rectangular cuboid, and its dimensions were determined based on the rotor diameter (D = 126 m) of the NREL 5MW wind turbine to ensure that the wake can fully develop without being affected by the domain boundaries. The specific dimensions of the domain are $L_x \times L_y \times L_z = 24D \times 8D \times 8D$, where L_x, L_y, and L_z are the lengths of the domain in the streamwise (x), cross-flow (y), and vertical (z) directions, respectively. Converted to actual values, the domain dimensions are 3024 m × 1008 m × 1008 m, with the inflow direction aligned with the positive x-axis.

In addition, to facilitate the analysis of the wake flow field, the coordinate system was defined as follows: the origin of the coordinate system is located at the center of the turbine rotor plane (i.e., the intersection point of the rotor axis and the rotor plane), the x-axis is along the streamwise direction (inflow direction), the y-axis is along the cross-flow direction (horizontal perpendicular to the inflow), and the z-axis is along the vertical direction (upward). The hub height of the turbine (90 m) corresponds to z = 90 m in this coordinate system.

To maintain the physical consistency of the flow field and ensure the stable development of the neutral ABL and wake, the boundary conditions of the computational domain were carefully prescribed as follows:

- Streamwise boundaries (x = 0 and x = 24D): Cyclic boundary conditions were applied to ensure the periodicity of the flow field in the streamwise direction, which is consistent with the infinite extension characteristics of the atmospheric boundary layer in practical scenarios;
- Cross-flow boundaries (y = 0 and y = 8D): Cyclic boundary conditions were also adopted to eliminate the influence of boundary reflection on the wake expansion, ensuring that the wake can freely develop in the cross-flow direction;
- Vertical boundaries (z = 0 and z = 8D): The lower boundary (z = 0)

was set as a solid wall, and the Moeng shear-stress model (Moeng 1984) was employed to accurately simulate the surface shear stress, which is critical for the development of the neutral ABL. The upper boundary (z = 8D) was set as a slip boundary to simulate the free atmosphere above the ABL, avoiding the influence of artificial boundary constraints on the vertical flow of the ABL.

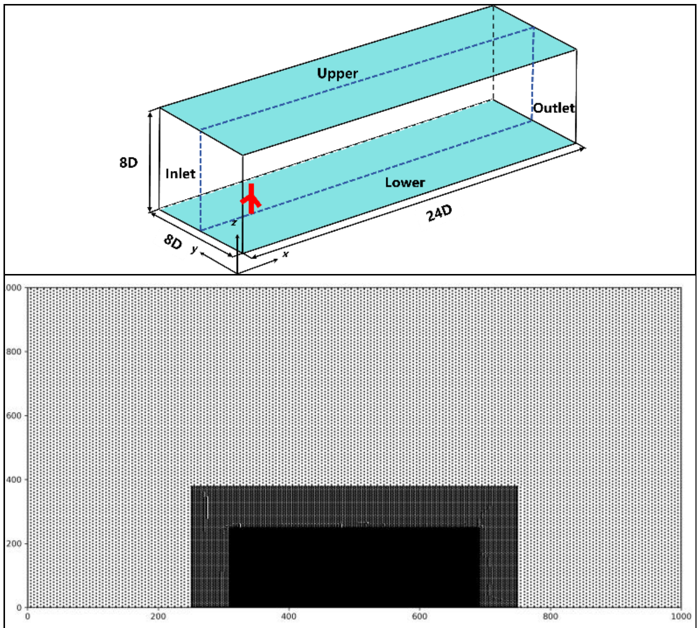

Figure 2. Illustration of the computational domain and grid.

Unstructured grids were generated for the computational domain. As shown in Fig. 2, grid refinement was implemented in the vicinity of the turbine and the wake region, and a two-stage gradual refinement strategy was adopted for the refined zones to avoid numerical errors induced by abrupt grid changes. The heights of the two refined zones were set to 2D and 3D (where D denotes the rotor diameter), respectively. The grid size of the secondary refined zone was 2.5 m × 2.5 m × 2.5 m, with the total number of grid points reaching 12 million. The wind turbine simulation was conducted for a duration of 1000 s with a time step of 0.02 s.

The grid convergence was verified through a series of grid sensitivity tests, ensuring that the grid size adopted in this study is sufficient to obtain grid-independent results.

The Reynolds numbers in the simulation were defined based on the bulk velocity and friction velocity to characterize the turbulent intensity of the flow field. The bulk Reynolds number Re_b was set to 20000, which is defined as $Re_b = \frac{U_b \delta}{\nu} = 20000$, where U_b is the bulk velocity of the flow field, δ is the channel half-height, and ν is the kinematic viscosity of air. These Reynolds number settings are consistent with the turbulent characteristics of the neutral ABL in practical wind farm scenarios, ensuring that the simulated flow field has realistic turbulence intensity.

CFD Results

The primary purpose of the CFD simulation is to generate high-fidelity wind turbine wake flow field data for training and validating the U-Net super-resolution model. Before using the simulation data, the accuracy and reliability of the CFD results were verified and validated through detailed comparisons with existing numerical results, which have been comprehensively discussed in the authors' previous work (omitted here for brevity).

Fig. 3 shows the velocity component U (streamwise velocity) distributions on the vertical slice of the computational domain at different streamwise positions (1D, 5D, and 9D downstream of the turbine rotor). These snapshots clearly illustrate the evolution characteristics of the wind turbine wake under neutral ABL conditions. At 1D downstream (Fig. 3a), a significant velocity deficit region appears directly behind the turbine rotor, which is the core region of the wake. The velocity in this region is significantly lower than the inflow velocity (11.4 m/s), and the velocity gradient is large, indicating strong shear effects between the wake and the surrounding undisturbed flow. As the wake propagates downstream to 5D (Fig. 3b), the wake begins to expand in the cross-flow and vertical directions, the velocity deficit region gradually expands, and the velocity gradient decreases, which is due to the turbulent mixing between the wake and the surrounding flow. At 9D downstream (Fig. 3c), the wake continues to expand, the velocity deficit is further reduced, and the wake boundary becomes blurred, but the core velocity deficit region is still visible, indicating that the wake has not yet fully recovered to the inflow velocity.

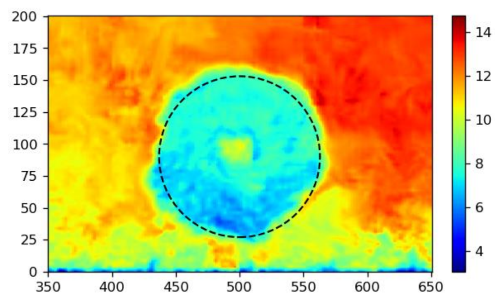

(a) 1D

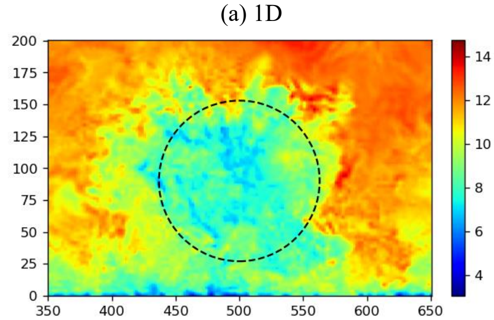

(b) 5D

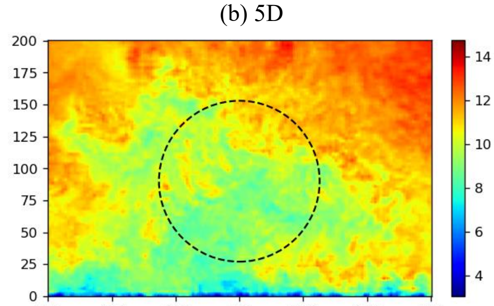

(c) 9D

Figure 3. LES results, i.e. the HR flow field. Colormap unit: m/s.

The CFD simulation generated a total of 300 s of continuous flow field data (18000–18300 s), with a time step of 0.1 s, resulting in 3000 flow field snapshots. Each snapshot contains the velocity components (U, V, W) and turbulence intensity data at all grid points in the computational domain. These data cover the entire process of wake evolution from the near-wake (1D) to the middle-wake (9D) region, and contain rich fine-scale flow features (such as wake vortices, shear layers, and turbulence structures), which are ideal training data for the U-Net super-resolution model.

In the subsequent model training, the streamwise velocity component U was selected as the key parameter for wake reconstruction, as it is the most critical parameter for evaluating wake characteristics and power loss in wind farms. The high-fidelity CFD data generated in this study not only provide a reliable ground truth for the super-resolution model but also ensure that the trained model can capture the complex nonlinear dynamic characteristics of wind turbine wakes under realistic atmospheric boundary layer conditions.

DEFINITION OF NN MODEL FOR SR OF WIND TURBINE WAKE FROM SPARSELY MEARUED DATA

Problem Definition

In this study, the mapping relationships to be established by the U-Net model are formulated in Eq. (6). Where U^{HR} denotes the high-resolution wind turbine wake field (ground truth from CFD simulations), and U^{LR} represents the low-resolution wake field obtained by down-sampling the CFD data. The formula aims to establish a nonlinear mapping between low-resolution input and high-resolution output through the U-Net model, realizing super-resolution reconstruction of wind turbine wake fields.

$$(U^{HR}) = \boldsymbol{U - Net}(U^{LR}) \tag{6}$$

The Neural Network Model for SR

U-Net is a CNN-based Encoder-Decoder model (Ronneberger et al. 2015). Widely used in image segmentation and super-resolution tasks due to its strong capability in capturing fine-grained features and restoring spatial details (Deng et al. 2019). As shown in Fig.4, it consists of an encoder, a decoder, and skip connections: the encoder extracts multi-scale feature information from low-resolution inputs through convolution and max-pooling; the decoder up-samples the features to recover high-resolution outputs; skip connections connect the encoder and decoder of the same scale to transmit detailed spatial information, avoiding feature loss during down-sampling.

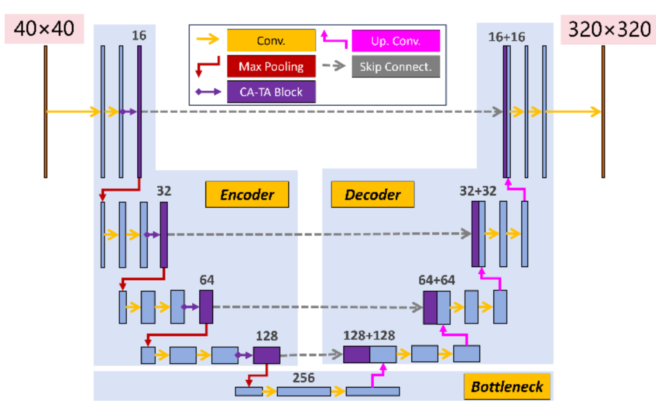

Figure 4. Illustration of U-Net.

In this work, the input is low resolution wind turbine wake field, output is high-resolution turbine wake field. U-Net is used to learn the nonlinear mapping between U^{LR} and U^{HR}, effectively restoring fine-scale flow features (e.g., wake vortices, velocity gradients) that are lost in low-resolution data.

MODEL TRAINING

To train the proposed U-Net model for wind turbine wake super-resolution (SR), the high-fidelity CFD dataset generated in Section 2 was processed systematically. This section details the key steps of model training, including data down-sampling, dataset splitting, and training specifications, ensuring the model can learn the nonlinear mapping between low-resolution (LR) and high-resolution (HR) wake fields effectively.

Data down-sampling

Consistent with the research design, two down-sampling rates (DSR = 16 and DSR = 32) were adopted to generate LR wake field data from the HR CFD data. The down-sampling process was implemented by averaging the HR streamwise velocity (U^{HR}) values within each DSR× DSR grid cell, which simulates the sparse and low-resolution measurements from practical lidar systems. Both DSR settings were applied to the same CFD dataset to ensure comparability of model performance. After down-sampling, the LR data retained the macro wake characteristics while losing fine-scale features (e.g., small vortices, local velocity gradients), which the U-Net model was required to reconstruct. Figs. 5(a), 5(b), and 5(c) show the original ground truth field, the field at DSR = 16, and the field at DSR = 32, respectively.

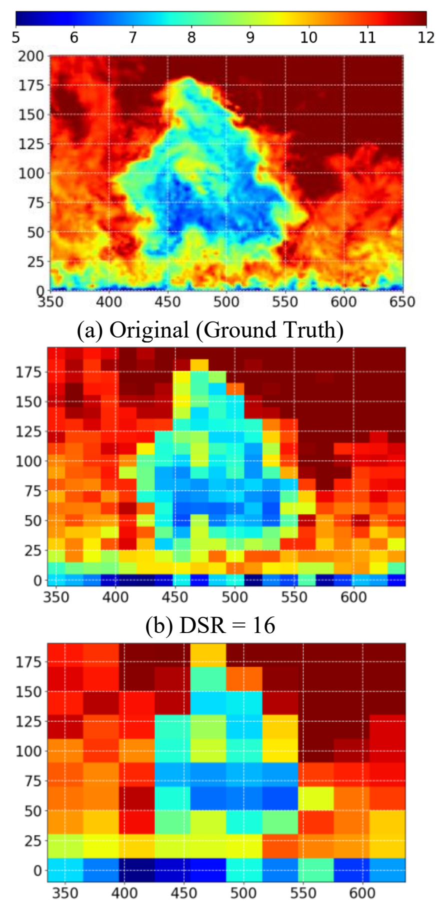

Figure 5. Illustration of data down-sampling. Colormap unit: m/s.

Dataset Splitting

The processed dataset (including HR and corresponding LR data under two DSRs) was randomly split into three subsets: training set, validation set, and test set, with a ratio of 7:2:1. The training set (70% of total data) was used to optimize the model parameters; the validation set (20%) was employed to monitor training progress and prevent overfitting; the test set (10%) was used to evaluate the final performance of the trained model objectively. To avoid data leakage, the three subsets were split without overlap, and the same splitting strategy was applied to both DSR = 16 and DSR = 32 datasets, ensuring consistent evaluation standards.

Training Specification

The U-Net model was trained using the PyTorch framework (Paszke et al. 2019), with the Adam optimizer selected for parameter updating due to its efficiency in convergence. The mean squared error (MSE) was adopted as the loss function, which measures the pixel-wise difference between the model-predicted HR wake field and the true HR CFD data, expressed as Eq. (7):

$$E_{RMS} = \sqrt{\frac{1}{m}\sum_{i=1}^{m}\left(y_i - y_i^{pred}\right)^2} \tag{7}$$

All neural network architectures utilized the Rectified Linear Unit (*ReLU*) activation function specified in Eq. (8) for hidden layers, which introduces non-linearity while maintaining computational efficiency through its piecewise linear operation. This activation choice facilitates gradient flow during backpropagation and mitigates vanishing gradient issues common in deep architectures. The final output layer employed linear activation to enable continuous velocity predictions without range constraints.

$$ReLU(x) = max(0, x) \tag{8}$$

The training batch size was set to 8, and the initial learning rate was 1×10^{-4}, which was reduced by half every 50 epochs to promote convergence. The model was trained for a total of 200 epochs, and early stopping was adopted (patience = 10) to prevent overfitting—training stopped if the validation loss did not decrease for 10 consecutive epochs. All training processes were conducted on a NVDIA GTX 3060 GPU to improve computational efficiency. Fig. 6(a) and 6(b) show the training loss histories for the models at DSR = 16 and 32, respectively.

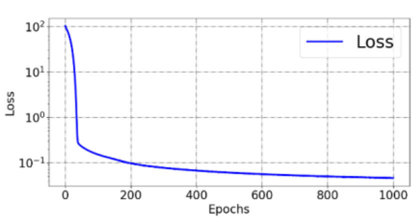

(a) DSR = 16

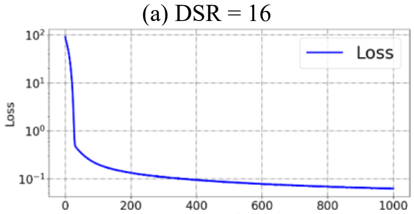

(b) DSR = 32

Figure 6. Histories of losses in the training process.

RESULTS AND DISCUSSION

DSR of 16

Each row in Fig. 7 corresponds to four types of flow field results, respectively: the low-resolution (LR) wake field (generated by 16×16 down-sampling of CFD data), the super-resolution (SR) result obtained by bicubic interpolation, the SR result reconstructed by the U-Net model, and the high-fidelity ground truth from CFD simulations. The left column displays the reconstruction performance on the training set, while the right column presents the results on the independent testing set, which is critical for evaluating the model's generalization ability.

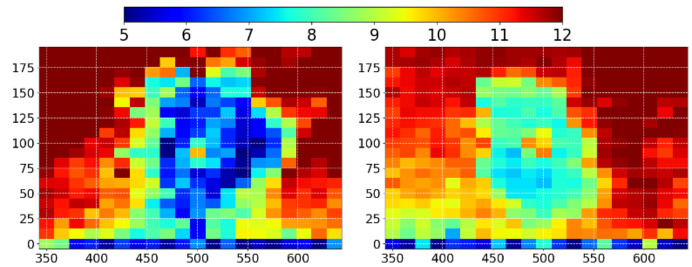

(a) LR (Training Set) (b) LR (Testing Set)

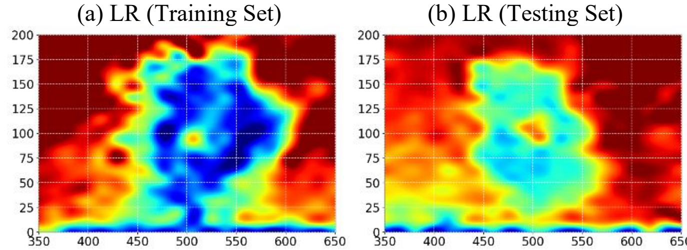

(c) Bi-cubic (Training Set) (d) Bi-cubic (Testing Set)

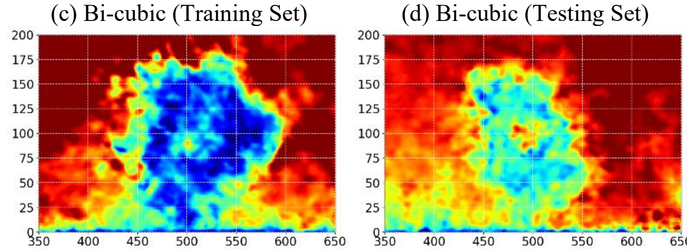

(e) U-Net (Training Set) (f) U-Net (Testing Set)

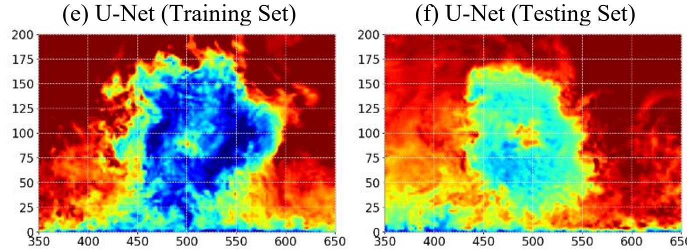

(g) Ground Truth (Training Set) (h) Ground Truth (Testing Set)

Figure 7. Super-resolution reconstruction of the wind turbine wake at DSR = 16. Colormap unit: m/s.

It is evident that the U-Net model outperforms bicubic interpolation significantly in SR reconstruction, both on the training and testing sets. Specifically, bicubic interpolation produces a overly smoothed flow field, failing to capture key fine-scale features such as small-scale wake vortices, local velocity gradients, and the sharp boundary of the velocity deficit region. In contrast, the U-Net model not only restores the overall structure of the wake but also effectively reconstructs these detailed flow characteristics, which are consistent with the ground truth. This advantage is particularly obvious in the near-wake region, where the velocity gradient is large: the U-Net can accurately reproduce the intensity and distribution of the velocity deficit, while bicubic interpolation blurs these critical physical features. Notably, the U-Net also performs well on the testing set, indicating that it has learned the inherent nonlinear mapping between LR and HR wake fields rather than simply overfitting the training data, which verifies its good generalization ability.

DSR of 32

To further test the robustness of the proposed U-Net model under more challenging conditions, the DSR was doubled from 16 to 32. Following the same layout as Fig. 7, each row in Fig. 8 corresponds to the LR field, SR result by bicubic interpolation, SR result by U-Net, and ground truth, with the left column showing performance on the training set and the right column on the testing set. A direct comparison between the LR fields under DSR = 32 (Figs. 8a and 8b) and DSR = 16 clearly reveals that the sampling points of the flow field under DSR = 32 are significantly sparser, such as the core velocity deficit region are barely distinguishable. This increased sparsity poses a greater challenge for SR reconstruction, as more fine-scale flow information is lost during the down-sampling process.

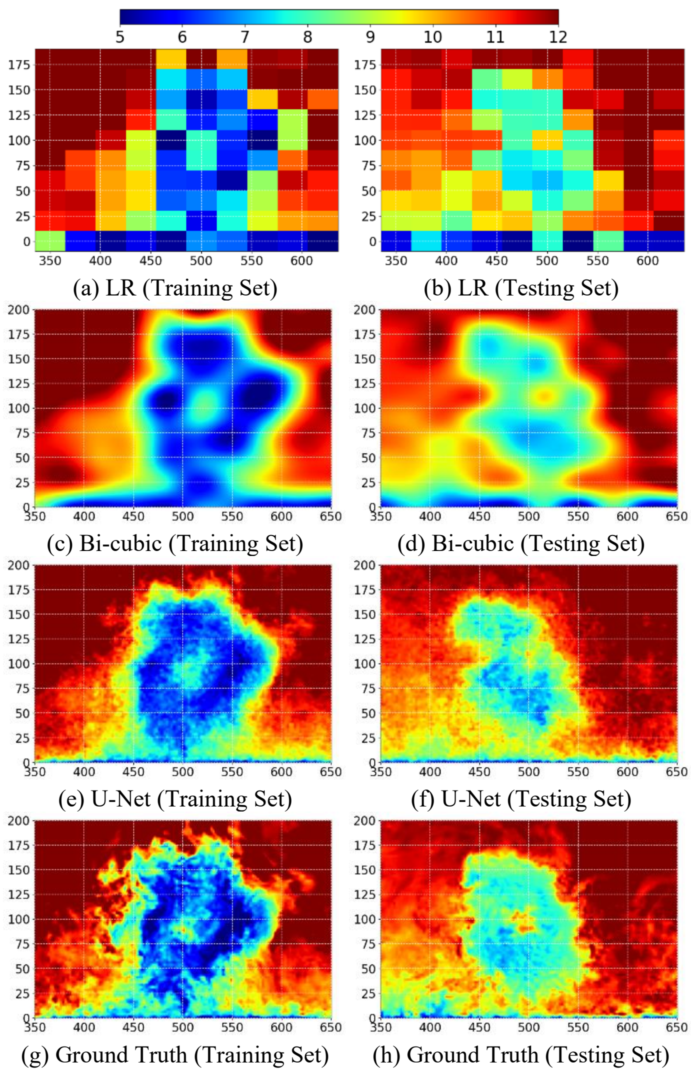

Figure 8. Super-resolution reconstruction of the wind turbine wake at DSR = 32. Colormap unit: m/s.

Even under this more challenging DSR = 32 scenario, the U-Net model still outperforms bicubic interpolation by a substantial margin, maintaining the advantage observed under DSR = 16. Specifically, bicubic interpolation only performs a simple smoothing operation on the sparse LR flow field, rather than truly reconstructing the lost flow features. It merely restores the "largest"-scale wake structures, such as the approximate shape of the velocity deficit region, but fails to capture any flow structures smaller than the interval of the sampling points—including small-scale vortices and local velocity gradients that are critical for accurate wake assessment. In contrast, the U-Net model, leveraging the nonlinear mapping learned from the high-fidelity CFD dataset, successfully reconstructs these smaller-scale flow features while preserving the overall wake structure. This demonstrates that the U-Net can effectively learn the inherent physical laws of wake evolution, even when the input data is highly sparse, which is consistent with its performance under DSR = 16 and further verifies its superiority over traditional interpolation methods.

Quantitative Evaluation

Quantitative validation employed two complementary metrics computed across all test samples: the spatially averaged root-mean-square error (E_{RMS}) and coefficient of determination (R^2). These metrics were calculated through ensemble averaging over the test samples as defined in Eq. (9) and Eq. (10):

$$\bar{E}_{RMS} = \frac{1}{TS}\sum_{j=1}^{TS} E_{RMS}^{j} \tag{9}$$

where TS is the total number of samples in the testing dataset, and for the jth cross section, or sample, E_{RMS}^{j} is defined as:

$$E_{RMS}^{j} = \sqrt{\frac{1}{N}\sum_{i=1}^{N}\left(u_i - u_i^{pred}\right)^2} \tag{10}$$

where N is the total number of points in one cross-section, i.e. $N = 320 \times 320$ in the present study, u_i is the velocity obtained by CFD, i.e. the ground truth, and u_i^{pred} is the velocity predicted by the NN models. R^2 is defined as:

$$\overline{R^2} = \frac{1}{TS}\sum_{j=1}^{TS}\left(R^2{}_j\right) \tag{11}$$

where, similarly, for the *j*-th cross section, or sample, $R^2{}_j$ is defined as:

$$R^2{}_j = 1 - \frac{\sum_{i=1}^{N}\left(u_i - u_i^{pred}\right)^2}{\sum_{i=1}^{N}\left(u_i - \overline{u_i}\right)^2} \tag{12}$$

It should be noted that the range of R^2-score is any value below (or equal to) 1, and a value closer to 1 indicates a higher accuracy of fit for the model.

To objectively verify the superiority of the U-Net model in wake SR reconstruction and quantify its performance under different down-sampling rates, two evaluation metrics were adopted: coefficient of determination (R^2) and root mean square error (E_{RMS}). R^2 reflects the consistency between the reconstructed flow field and the ground truth (closer to 1 indicates better consistency), while E_{RMS} measures the reconstruction error (smaller values indicate higher accuracy). Both metrics were calculated based on the streamwise velocity component (U), the core parameter for characterizing wake features.

Table 1 summarizes the quantitative results of the U-Net model and bicubic interpolation on both the training set and testing set under DSR = 16 and DSR = 32. All metrics were averaged over all flow field snapshots in the corresponding testing datasets to ensure statistical reliability.

Table 1. The values of R^2 / E_{RMS} (m/s) for different SR approaches.

DSR	Bi-cubic	U-Net
16	-10.32 / 4.01 (m/s)	0.83 / 1.53 (m/s)
32	-15.22 / 7.23 (m/s)	0.69 / 2.29 (m/s)

The quantitative results in Table 1 are consistent with the qualitative observations. Under both DSR settings, the U-Net model outperforms bicubic interpolation significantly. At DSR = 16, U-Net achieves an R^2 of 0.83 and E_{RMS} of 1.53 (m/s), much better than bicubic interpolation (R^2 = 0.32, E_{RMS} = 4.01 (m/s)), indicating higher consistency and lower reconstruction error. When DSR increases to 32, bicubic interpolation performs drastically worse (R^2 = -15.22, E_{RMS} = 7.23 (m/s)), failing to capture the flow field structure. In contrast, U-Net maintains acceptable performance (R^2 = 0.69, E_{RMS} = 2.29 (m/s)), with only a slight decrease from DSR = 16, verifying its robustness in handling highly sparse input data.

CONCLUSIONS

This study focuses on the problem of reconstructing high-fidelity wind turbine wake fields from sparse, low-resolution measurement data. To address this issue, a high-fidelity CFD dataset was first generated, which simulates the wake characteristics of the NREL 5MW wind turbine operating in a neutral atmospheric boundary layer (ABL) using a two-stage Large Eddy Simulation (LES) strategy. Subsequently, a U-Net model was adopted for super-resolution (SR) reconstruction, with two down-sampling rates (DSR = 16 and DSR = 32) designed to simulate sparse lidar measurements. The model was trained using the CFD dataset, and its performance was comprehensively evaluated through qualitative and quantitative comparisons with the traditional bicubic interpolation method.

The key innovations and main conclusions of this work are as follows: first, it is the first attempt to integrate deep learning-based super-resolution technology with wind turbine wake monitoring, realizing the reconstruction of high-fidelity wake fields from sparse low-resolution data. Second, the quantitative and qualitative results consistently show that the U-Net model significantly outperforms bicubic interpolation under both DSR settings: at DSR = 16, the U-Net achieves an R^2 of 0.83 and E_{RMS} of 1.53 (m/s), much better than bicubic interpolation (R^2 = 0.32, E_{RMS} = 4.01 (m/s)); at the more challenging DSR = 32, bicubic interpolation fails completely (R^2 = -15.22, E_{RMS} = 7.23 (m/s)), while the U-Net still maintains acceptable performance (R^2 = 0.69, E_{RMS} = 2.29 (m/s)), demonstrating strong robustness. Third, the U-Net model can effectively reconstruct fine-scale flow features (e.g., small vortices, velocity gradients) that are lost in low-resolution data, which is crucial for accurate wake assessment and wind farm operational optimization.

For future research, several directions can be further explored. First, the proposed method can be extended to non-neutral atmospheric boundary layer conditions (e.g., stable or unstable ABL) to enhance its applicability in complex real-world atmospheric environments. Second, the model can be validated using actual lidar measurement data from wind farms, bridging the gap between numerical simulation and practical engineering applications. Third, the U-Net model can be optimized by introducing more advanced network structures or loss functions to further improve reconstruction accuracy and computational efficiency. Finally, the method can be expanded to multi-turbine array scenarios, providing technical support for large-scale wind farm wake management and power generation optimization.

ACKNOWLEDGEMENT

This work was supported by the National Key Research and Development Program of China (2025YFF0515700), to which the authors are most grateful.

REFERENCES

Amiri, MM, Shadman, M, and Estefen, SF (2024). "A review of physical and numerical modeling techniques for horizontal-axis wind turbine wakes," *Renew Sustain Energy Rev*, 193, 114279.

Bastankhah, M, and Porté-Agel, F (2014). "A new analytical model for wind-turbine wakes," *Renew Energy*, 70, 116–123.

Chen, M (2023). "Super-resolution reconstruction framework of wind turbine wake: Design and application," *Ocean Eng*, 288, 116099.

Chen, Y, Wang, D, Feng, D, Tian, G, Gupta, V, Cao, R, Wan, M, and Chen, S (2025). "Three-dimensional spatiotemporal wind field reconstruction based on LiDAR and multi-scale PINN," *Appl Energy*, 377, 124577.

Deng, Z, He, C, Liu, Y, and Kim, KC (2019). "Super-resolution reconstruction of turbulent velocity fields using a generative adversarial network-based artificial intelligence framework," *Phys Fluids*, 31(12), 125111.

Jonkman, J, Butterfield, S, Musial, W, and Scott, G (2009). Definition of a 5-MW reference wind turbine for offshore system development.

Lecun, Y, Bengio, Y, and Hinton, G (2015). "Deep learning," *Nature*, 521(7553), 436–444.

Lee, S, Churchfield, M, Moriarty, P, Jonkman, J, and Michalakes, J (2012). "Atmospheric and Wake Turbulence Impacts on Wind Turbine Fatigue Loadings," *In: Proc 50th AIAA Aerospace Sciences Meeting including the New Horizons Forum and Aerospace Exposition*, American Institute of Aeronautics and Astronautics, Nashville, Tennessee.

Moeng, C-H (1984). "A Large-Eddy-Simulation Model for the Study of Planetary Boundary-Layer Turbulence," *J Atmospheric Sci*, 41(13), 2052–2062.

Paszke, A, Gross, S, Massa, F, Lerer, A, Bradbury, J, Chanan, G, Killeen, T, Lin, Z, Gimelshein, N, Antiga, L, Desmaison, A, Kopf, A, Yang, E, DeVito, Z, Raison, M, Tejani, A, Chilamkurthy, S, Steiner, B, Fang, L, Bai, J, and Chintala, S (2019). "PyTorch: An Imperative Style, High-Performance Deep Learning Library," *In: Proc 33rd International Conference on Neural Information Processing Systems (NeurIPS 2019)*, Curran Associates, Inc., Red Hook, NY, USA.

Ronneberger, O, Fischer, P, and Brox, T (2015). U-Net: Convolutional Networks for Biomedical Image Segmentation.

Sørensen, JN, and Shen, WZ (2002). "Numerical Modeling of Wind Turbine Wakes," *J Fluids Eng*, 124(June 2002), 393–399.

Xu, S, Xue, Y, Zhao, W, and Wan, D (2022). "A Review of High-Fidelity Computational Fluid Dynamics for Floating Offshore Wind Turbines," *J Mar Sci Eng*, 10(10).

Ye, M, Chen, H-C, and Koop, A (2023). "High-fidelity CFD simulations for the wake characteristics of the NTNU BT1 wind turbine," *Energy*, 265(November 2022), 126285.

Ye, M, Chen, H-C, and Koop, A (2024). "High-fidelity CFD simulations of two tandemly arrayed wind turbines under various operating conditions," *Ocean Eng*, 314, 119703.

Ye, M, Fan, G, and Wan, D (2025). "Enhancing turbulent channel flow super-resolution via physics-guided deep learning with global pressure correlations," *J Hydrodyn*.

Ye, M, Zhong, Y, Chen, H-C, and Wan, D (2026). "Investigating the impact of numerical uncertainties in CFD-generated training data on neural network models for wind-turbine wake predictions," *Ocean Eng*, 343, 123200.